

Article

DFT Investigation on the Complexation of β -Cyclodextrin and Hydroxypropyl- β -Cyclodextrin as Recognition Hosts with Trichloroethylene

Ahlem Benmerabet ^{1,2}, Abdelaziz Bouhadiba ¹, Youghourta Belhocine ¹ , Seyfeddine Rahali ³ , Najoua Sbei ⁴, Mahamadou Seydou ^{5,6,*} , Ihsene Boucheriha ¹, Imane Omeiri ¹ and Ibtissem Meriem Assaba ^{1,2} 

- ¹ Laboratory of Catalysis, Bioprocess and Environment, Department of Process Engineering, Faculty of Technology, University of 20 August 1955, Skikda 21000, Algeria; ispprof94@gmail.com (A.B.); a.bouhadiba@univ-skikda.dz (A.B.); y.belhocine@univ-skikda.dz (Y.B.); ihseneboucheriha21@gmail.com (I.B.); imaneomeiri99@gmail.com (I.O.); ibtissem1994assaba@gmail.com (I.M.A.)
- ² LRPCSI-Laboratoire de Recherche sur la Physico-Chimie des Surfaces et Interfaces, University of 20 August 1955, Skikda 21000, Algeria
- ³ Department of Chemistry, College of Science and Arts At Ar-Rass, Qassim University, Saudi Arabia; saif.rahali@gmail.com
- ⁴ Institute of Nanotechnology, Karlsruhe Institute of Technology, Eggenstein Leopoldshafen, 76344 Karlsruhe, Germany; najwasbei89@hotmail.fr
- ⁵ Université Paris Cité, CNRS, ITODYS, F-75013 Paris, France
- ⁶ Université des Sciences, des Techniques et des Technologies de Bamako (USTTB), Bamako BP 423, Mali
- * Correspondence: mahamadou.seydou@univ-paris-diderot.fr

Abstract: In this investigation, the potential use of native β -cyclodextrin (β -CD) and hydroxypropyl- β -cyclodextrin (HP- β -CD) as encapsulating agents for trichloroethylene (TCE) was assessed. Various quantum chemical parameters, including HOMO, LUMO, and HOMO–LUMO gap, were calculated. The docking process was examined by considering different initial configurations. The complexation energies were calculated at the molecular level using DFT/BLYP-D4 and PBEh-3c calculations to gain insight into TCE encapsulation within the β -CD and HP- β -CD cavities. We used the independent gradient model (IGM) and extended charge decomposition analysis (ECDA) approaches to examine non-covalent interactions and charge transfer within TCE@ β -CD and TCE@HP- β -CD complexes. The calculated thermodynamic data and complexation energies exhibited negative values for both considered complexes, indicating a favorable complexation process. Weak Van der Waals intermolecular interactions were the main driving forces in stabilizing the formed complex. Additionally, Monte Carlo simulations were conducted for a better understanding of the inclusion process. Our results provide evidence for the use of β -CD and HP- β -CD as suitable macrocyclic hosts for complexing trichloroethylene.

Keywords: β -cyclodextrin; hydroxypropyl- β -cyclodextrin; trichloroethylene; non-covalent interactions; density functional theory; Monte Carlo simulations



Citation: Benmerabet, A.; Bouhadiba, A.; Belhocine, Y.; Rahali, S.; Sbei, N.; Seydou, M.; Boucheriha, I.; Omeiri, I.; Assaba, I.M. DFT Investigation on the Complexation of β -Cyclodextrin and Hydroxypropyl- β -Cyclodextrin as Recognition Hosts with Trichloroethylene. *Atoms* **2023**, *11*, 153. <https://doi.org/10.3390/atoms11120153>

Academic Editor: Alexander Alijah

Received: 1 October 2023

Revised: 24 November 2023

Accepted: 1 December 2023

Published: 7 December 2023



Copyright: © 2023 by the authors. Licensee MDPI, Basel, Switzerland. This article is an open access article distributed under the terms and conditions of the Creative Commons Attribution (CC BY) license (<https://creativecommons.org/licenses/by/4.0/>).

1. Introduction

Supramolecular chemistry is a relatively recent branch of chemistry [1]. It was first introduced in 1967 by Pedersen, Lehn, and Cram during their discovery of crown ethers, an achievement that earned them the Nobel Prize in Chemistry in 1987 [2]. This field, also known as the chemistry of complex matter [3], primarily focuses on the phenomena of inclusion and capture of molecules, enabling the construction of new structures through the molecular assembly of chemical entities via weak, reversible, and non-covalent intermolecular interactions [4]. In recent years, inclusion complexes have garnered significant interest, particularly those formed with host macrocyclic systems such as crown ethers [5],

cucurbit[n]urils [6], cyclodextrins [7], and calix[n]arenes [8]. The study of inclusion complexation involving cyclodextrins and their derivatives has particularly gained increasing attention due to their versatile properties, making them suitable for various applications in environmental protection, food, pharmaceuticals, and cosmetics industries [9–13].

Cyclodextrins (CDs) are a class of natural cyclic oligosaccharides that are widely recognized as host molecules [14–16], made up of 6–12 glucopyranose units linked by α -(1,4) linkages. The three common cyclodextrins are α -cyclodextrin (α -CD), β -cyclodextrin (β -CD), and γ -cyclodextrin (γ -CD), composed of six, seven, and eight glucopyranose units, respectively [17]. CDs have truncated cone-like structures with a hydrophobic interior cavity and a hydrophilic exterior surface [18,19]. Hydroxypropyl- β -cyclodextrin (HP- β -CD) is a chemically modified derivative of β -CD with a similarly sized cavity and enhanced aqueous solubility due to its strong hydrophilicity, thus enabling the formation of soluble inclusion complexes [20].

Chlorinated hydrocarbon solvents, including trichloroethylene, tetrachloroethylene, 1,1,1-trichloroethane, 1,2-dichloroethane, and carbon tetrachloride, are often detected in surface waters due to their volatility. Among them, trichloroethylene (TCE) stands out as a widely used non-flammable volatile organic compound known for its poor water solubility. It is employed in a range of industries, households, and even water treatment plants.

TCE has emerged as a significant global public health and environmental concern. It is recognized as a prevalent environmental pollutant affecting groundwater, soil, and air, particularly in heavily industrialized regions due to processes such as wastewater discharge, volatilization, combustion, and pesticide use. Long-term human exposure to TCE increases the risk of cancer [21–23] and poses serious threats to biological systems and living organisms. TCE is listed 16th on the United States Environmental Protection Agency's priority list of hazardous substances and ranks 3rd according to the Ministry of Ecology and Environment of the People's Republic of China [24]. Several methods have been developed for remediating TCE-contaminated groundwater, with carbon adsorption being a common technique for TCE removal.

During the last decades, remediation efforts for chlorinated hydrocarbon solvents such as trichloroethylene (TCE) have evolved. Numerous methods, including aeration, adsorption, and boiling water that contains volatile organic solvents, have been employed [25]. Catalytic hydrodechlorination, particularly using palladium (Pd), has gained popularity for effectively degrading a wide range of chlorinated compounds in both gas and liquid phases. Pd catalysis is known for its ability to cleave C–Cl bonds and generate reactive atomic hydrogen on its surface. The bio-Pd approach has been developed to produce nanopalladium catalysts by precipitating palladium on bacterial surfaces for dechlorination of trichloroethylene [26]. Nano-scale zero-valent iron (NZVI) has also emerged as an efficient reduction catalyst for the removal of TCE from groundwater due to its rapid degradation of chlorinated solvents.

Recently, there has been growing interest in supramolecular host systems, particularly those involving cyclodextrin and its polymers, for the remediation of environmental contaminants. In this regard, Xie et al. [27] have reported the advantageous use of porous β -cyclodextrin polymer for water purification. This approach aims to remove organic micro-pollutants and natural organic substances from water bodies while simultaneously eliminating pathogenic microorganisms. Functional hydrogel-based evaporators incorporating cyclodextrins have demonstrated exceptional performance in solar-driven water purification. As an illustration, Lin and his research group incorporated β -cyclodextrin (β -CD) into polyvinyl alcohol (PVA)-based hydrogels [28]. The hydrogel displayed an impressive adsorption capacity for Pb (II) and Ni (II), reaching 505.9 mg/g and 286.7 mg/g, respectively, with a water treatment efficiency exceeding 99% for low-concentration heavy metal ions. Additionally, Miao et al. [29] developed a hybrid hydrogel by incorporating β -CD to polyacrylamide (PAM). Similarly, Crini et al. [30] reported the functionalization and modification of carbon nanotubes (CNT) with β -cyclodextrin (β -CD), resulting in enhanced sensitivity for the detection of pharmaceuticals and organic micro-pollutants

such as rutin and bisphenol A. These high-aspect-ratio CNTs (>3000) provide a substantial effective surface area and strong redox capability, while β -CD facilitates and enhances host-guest interaction capabilities.

Computational chemistry has been recognized as a successful approach for studying and predicting a wide range of physicochemical properties such as simulating spectroscopic properties [31], exploring chemical reactivity [32], and rationalizing the host-guest interactions of supramolecular assemblies [33,34]. Host-guest complexes are of great interest to supramolecular chemistry due to the host's capacity to induce physicochemical changes in the properties of the guest molecules by improving their solubility, bioavailability, and stability [20]. Both experimental and theoretical methods are employed in a complementary manner to investigate the structural, electronic, and dynamical changes that occur during the inclusion process.

Numerous studies in the literature, including those conducted by Shirin et al. [35], Kashiyama et al. [36], Liang et al. [37], and Khan et al. [38], have reported the formation of inclusion complexes between cyclodextrins (and their derivatives) and chlorinated hydrocarbons.

The current investigation aimed to examine, using a theoretical approach based on the density functional theory (DFT) method, the capacity of β -cyclodextrin (β -CD) and hydroxypropyl- β -cyclodextrin (HP- β -CD) to form inclusion complexes with trichloroethylene (TCE). The energetic and electronic properties, as well as the nature of non-covalent interactions that play a pivotal role in the inclusion process, were examined.

2. Computational Details

Density functional theory computations were carried out using the ORCA program (version 5.0.0) [39,40]. The starting structure of β -CD was retrieved from its crystal structure [41], and the HP- β -CD structure was built by adding hydroxypropyl groups to β -CD. The full geometry optimization of the complexes formed between trichloroethylene (TCE) and the CDs (β -CD and HP- β -CD) was conducted in the gas phase by employing the BLYP-D4 functional [42–44], along with the def2-SVP basis set. To account for the basis set superposition error (BSSE), a geometrical counterpoise correction scheme (gCP) [45] was applied. The approach suggested by Liu and Guo was used [46] to create initial complexes. The center of the coordination system was set at 0 Å for both TCE and HP- β -CD or β -CD. Subsequently, the TCE molecule was systematically translated along the Z-axis from –8 to +8 Å with a step size of 2 Å, involving two possible inclusion modes: mode A, where TCE approached the wider rim of β -CD and HP- β -CD cavities by its ClCH group, and mode B, where it approached through the dichlorocarbene group (CCl₂). These modes are depicted in Figure 1 using the Jmol version 14.32.60 [47].

The most stable configurations correspond to structures with the lowest complexation energies. The complexation energies were computed using Equation (1):

$$\Delta E_{\text{Complexation}} = E_{\text{Complex (TCE@CD)}} - (E_{\text{TCE}} + E_{\text{CD}}) \quad (1)$$

where $\Delta E_{\text{Complexation}}$ represents the complexation energy, while $E_{\text{Complex (TCE@ HP-}\beta\text{-CD)}}$, E_{TCE} , and E_{CD} represent, respectively, the energies of the complex, the free TCE, and the free β -CD or HP- β -CD systems. The most stable structures were then subjected to further analysis, including charge decomposition analysis (CDA) and its extended version, ECDA [48–50], as well as non-covalent interaction (NCI) analysis based on the independent gradient model (IGM) [51]. These analyses were performed using the wave function analysis code Multiwfn [52] and the VMD visualization program [53].

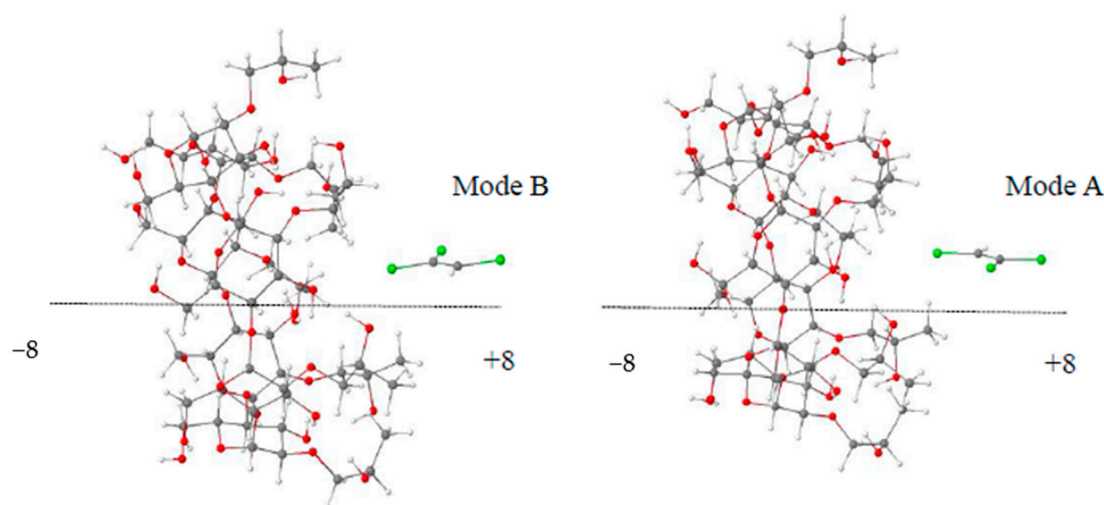


Figure 1. Coordinate systems describing the complexation process between HP- β -CD and TCE for A and B modes. Atomic color code: carbon (grey), hydrogen (white), oxygen (red), green (chlorine).

3. Results and Discussion

3.1. Calculations of Complexation Energies

The computed complexation energy values for TCE inclusion into β -CD and HP- β -CD in both A and B modes are presented in Table 1. For all the optimized TCE@ β -CD complexes, the complexation energy falls within the range of -14.20 kcal/mol to -18.44 kcal/mol, while, for TCE@HP- β -CD complexes, it varies between -12.50 and -21.21 kcal/mol. The negative complexation energies for all studied configurations indicate that the inclusion process is thermodynamically favorable. The most stable configurations, corresponding to the lowest energy, are found at $Z = -4$ Å in mode A for TCE@HP- β -CD and at $Z = -4$ Å in mode B for TCE@ β -CD, with complexation energy values of -21.21 and -18.44 kcal/mol, respectively. This suggests that the inclusion process is more favorable for the formation of the TCE@HP- β -CD complex in the gas phase. The addition of nonpolar substituents in the CD host can strengthen binding through hydrophobic interactions with nonpolar guest molecules. However, the binding affinity between HP- β -CD and TCE seems to be slightly stronger than that between β -CD and TCE, possibly due to the steric hindrance introduced by the hydroxypropyl groups in HP- β -CD [35].

Table 1. The complexation energies between TCE and the cyclodextrins (β -CD and HP- β -CD) computed at BLYP-D4/def2-SVP-gCP level (kcal/mol) in the gas phase.

| Inclusion Configurations | TCE@ β -CD Mode A | TCE@ β -CD Mode B | TCE@HP- β -CD Mode A | TCE@HP- β -CD Mode B |
|--------------------------|-------------------------|-------------------------|----------------------------|----------------------------|
| -8 | -12.21 | -16.42 | -12.51 | -14.04 |
| -6 | -16.73 | -16.49 | -12.50 | -13.55 |
| -4 | -16.73 | -18.44 | -21.20 | -15.78 |
| -2 | -16.73 | -16.80 | -16.53 | -15.78 |
| 0 | -17.77 | -16.78 | -16.54 | -16.28 |
| 2 | -14.42 | -17.30 | -16.43 | -17.12 |
| 4 | -14.44 | -14.20 | -16.63 | -14.87 |
| 6 | -12.38 | -15.72 | -16.72 | -12.77 |
| 8 | -12.82 | -15.49 | -12.95 | -14.71 |

Furthermore, the obtained structures underwent re-optimization using the composite method PBEh-3c [54] to enhance result accuracy. In the gas phase, the complexation energies were determined to be -20.34 and -13.09 kcal/mol for TCE@HP- β -CD and TCE@ β -CD, respectively. Meanwhile, in the aqueous phase, the complexation energies using the SMD solvation model [55] were found to be -14.97 and -15.02 kcal/mol, respectively. The

complexation energies calculated with PBEh-3c exhibit a similar trend to those obtained at the BLYP-D4/def2-SVP-gCP level. Consequently, the process of solvation led to an increase in the complexation energy between TCE and β -CD while causing a decrease in the complexation energy between TCE and the HP- β -CD host. Figure 2 shows the structural analysis of the most stable TCE@HP- β -CD complex in the gas phase, revealing the full inclusion of TCE inside the HP- β -CD cavity, thus contributing to the complex stabilization.

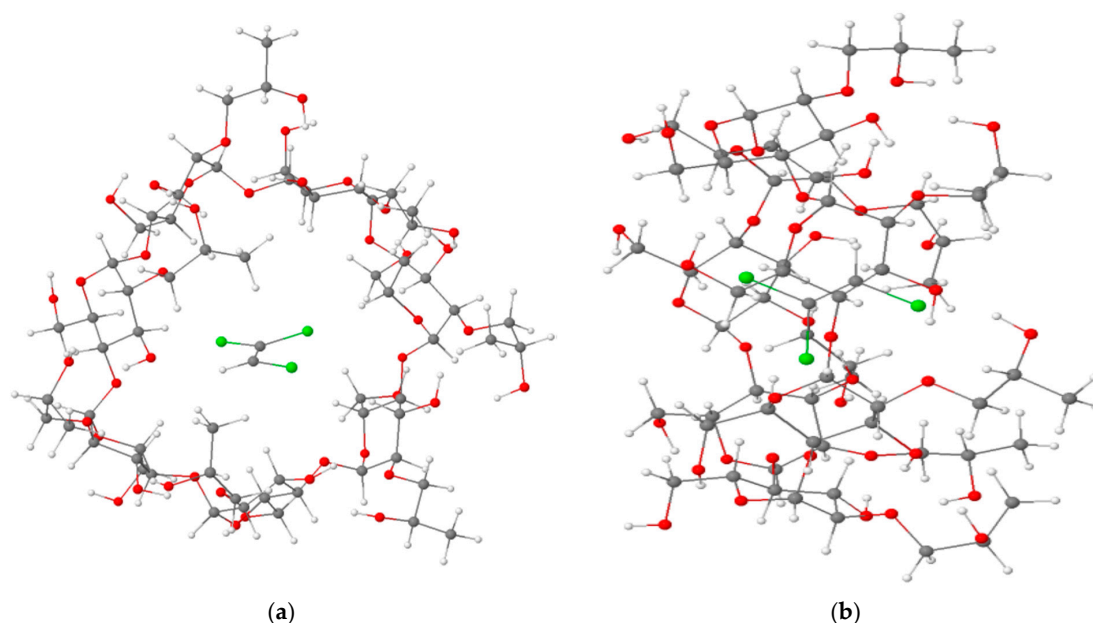


Figure 2. Front (a) and side (b) views of the full inclusion of TCE inside HP- β -CD of the most stable configuration of the formed complex (TCE@HP- β -CD). Atomic color code: carbon (grey), hydrogen (white), oxygen (red), green (chlorine).

3.2. Thermodynamics Properties of the Inclusion Processes

The thermodynamic properties of the inclusion processes of the most stable structures for TCE@HP- β -CD (−4A) and TCE@ β -CD (−4B) were calculated in the gas phase using the BLYP-D4/def2-SVP-gCP level of theory, including the ZPE correction. The energy values of the Gibbs free energy (ΔG°), enthalpy (ΔH°), and entropy T(ΔS°) are listed in Table 2. Negative ΔG° values for both TCE@HP- β -CD (−4A) and TCE@ β -CD (−4B) indicate that the inclusion complexation occurs spontaneously, with the former being more spontaneous (−5.02 kcal/mol). Furthermore, enthalpy and entropy changes exhibit negative values of −19.34 and −14.31 kcal/mol for TCE@HP- β -CD (−4A) and −16.08 and −14.29 kcal/mol for TCE@ β -CD (−4B), revealing that the inclusion process is enthalpically driven and exothermic in nature.

Table 2. The energetic parameters for TCE@HP- β -CD (−4A) and TCE@ β -CD (−4B) calculated at the BLYP-D4/def2-SVP-gCP level of theory in the gas phase.

| Energetic Parameters | TCE@HP- β -CD (−4A) | TCE@ β -CD (−4B) |
|---|---------------------------|------------------------|
| $\Delta E_{\text{complexation}}$ (kcal/mol) | −21.20 | −18.44 |
| ΔH° (kcal/mol) | −19.34 | −16.08 |
| ΔG° (kcal/mol) | −5.02 | −1.79 |
| T(ΔS°) (kcal/mol) | −14.31 | −14.29 |

3.3. DFT Calculations of HOMO, LUMO, HOMO–LUMO Energy Gap, and Dipole Moment

Quantum physicochemical parameters, including the energies of the highest occupied molecular orbital (HOMO) and lowest unoccupied molecular orbital (LUMO), the HOMO–LUMO gap, and the global dipole moment of the studied inclusion complexes

were calculated at PBEh-3c and BLYP-D4/def2-SVP-gCP levels of theory and are presented in Table 3. The HOMO–LUMO gaps (eV) for different considered configurations in both Modes A and B are provided in supplementary data (Table S1).

Table 3. Frontier orbitals, HOMO–LUMO gaps, and global dipole moments for β -CD, HP- β -CD, TCE, TCE@ β -CD, and TCE@HP- β -CD systems calculated at the PBEh-3c (values between parentheses) and BLYP-D4/def2-SVP-gCP levels of theory in gas and water solvent phases.

| Parameters | HP- β -CD | β -CD | TCE | TCE@HP- β -CD | TCE@ β -CD |
|--------------------------------------|-----------------|---------------|---------------|---------------------|------------------|
| E_{HOMO} (eV) (gas) | −5.18 (−7.88) | −5.24 (−8.06) | −5.78 (−8.15) | −5.37 (−8.07) | −5.32 (−8.18) |
| E_{HOMO} (eV) (water) | −5.27 (−8.07) | −5.55 (−8.34) | −5.72 (−8.09) | −5.26 (−8.07) | −5.57 (−8.21) |
| E_{LUMO} (eV) (gas) | −0.22 (2.24) | −0.59 (1.94) | −1.39 (−0.02) | −1.58 (−0.14) | −2.07 (−0.63) |
| E_{LUMO} (eV) (water) | 0.43 (2.44) | 0.50 (2.75) | −1.27 (0.10) | −1.48 (−0.02) | −1.49 (−0.07) |
| ΔE_{Gap} (eV) (gas) | 4.96 (10.12) | 4.65 (10.00) | 4.39 (8.13) | 3.79 (7.93) | 3.25 (7.55) |
| ΔE_{Gap} (eV) (water) | 5.70 (10.51) | 6.05 (11.09) | 4.45 (8.19) | 3.78 (8.05) | 4.08 (8.14) |
| μ (Debye) (gas) | 6.61 (6.48) | 9.39 (9.86) | 0.71 (0.93) | 7.30 (7.57) | 10.54 (10.79) |
| μ (Debye) (water) | 8.63 (9.95) | 10.84 (8.88) | 1.13 (1.39) | 10.71 (11.80) | 13.35 (13.26) |

PBEh-3c and BLYP-D4/def2-SVP-gCP calculations indicate that the HOMO–LUMO energy gaps of TCE@HP- β -CD and TCE@ β -CD are reduced in both the gas phase and in a water solvent, when compared with the isolated HP- β -CD and β -CD. This reduction suggests heightened reactivity and increased electronic conductivity. Therefore, HP- β -CD and β -CD may serve as host molecules for the development of effective chemical sensors for the detection of trichloroethylene (TCE).

The findings in Table 3 also indicate a correlation between the HOMO–LUMO gap and both kinetic stability and, consequently, complexation energies. Both BLYP-D4-gCP and PBEh-3c calculations depict that, in the gas phase, TCE@HP- β -CD exhibits a larger HOMO–LUMO gap than TCE@ β -CD, while, in a water solvent, the trend is reversed, with TCE@ β -CD having a smaller HOMO–LUMO gap than TCE@HP- β -CD.

The computed frontier orbitals HOMO and LUMO of the TCE@HP- β -CD complex were plotted and visualized using the AVOGADRO program [56] and are displayed in Figure 3.

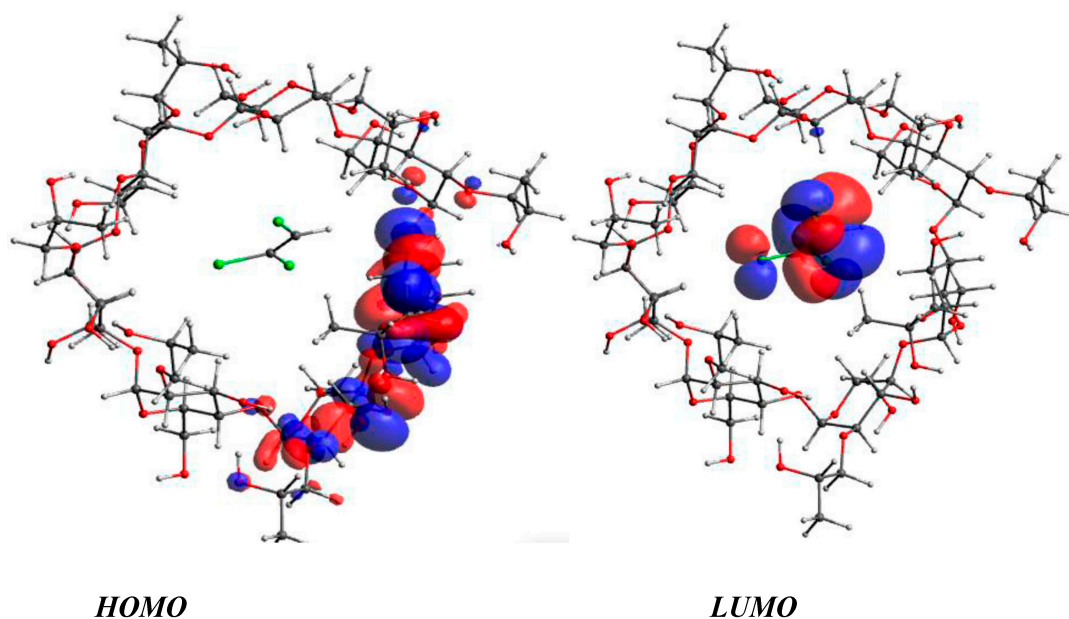


Figure 3. Frontier molecular orbitals HOMO and LUMO of the complex TCE@HP- β -CD.

It can be observed that the highest occupied molecular orbital (HOMO) is localized within a portion of the HP- β -CD host, whereas the lowest unoccupied molecular orbital (LUMO) is almost entirely delocalized over the TCE molecule.

3.4. Characterization of the Non-Covalent Intermolecular Interactions

To characterize the role and nature of noncovalent intermolecular interactions involved in stabilizing the TCE@HP- β -CD complex, the IGM methodology [57] based on Hirshfeld partition of molecular density (IGMH) was employed, allowing for a separation of intra- and intermolecular interactions. The IGM plots are color-coded to illustrate different intermolecular interactions. Red, green, and blue colors correspond to steric repulsion, weak Van der Waals, and hydrogen-bond interactions, respectively. Figure 4 depicts the IGM isosurface plot (0.002 a.u.) of the TCE@HP- β -CD complex using the VMD program. The topological analysis reveals that green areas predominate on the calculated isosurfaces [58–60], indicating the presence of weak Van der Waals interactions, which act as attractive forces between TCE and HP- β -CD, confirming their role in stabilizing the formed complex.

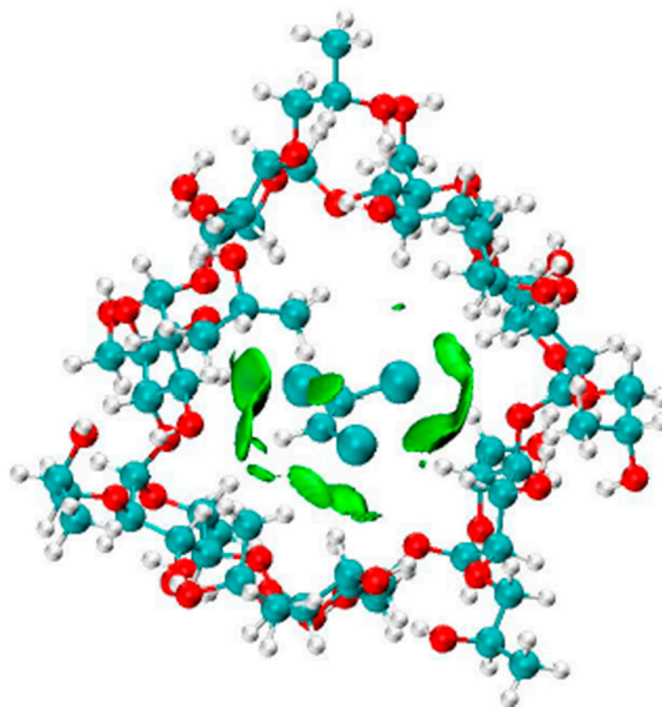


Figure 4. The IGM isosurface (isovalue 0.002 a.u.) of the TCE@HP- β -CD complex.

3.5. Charge Decomposition Analysis

Both the charge decomposition analysis (CDA) and the extended charge decomposition analysis (ECDA) are two methodologies that can be utilized to estimate the charge transfer occurring between fragments in host–guest complexes. Multiwfn code was used to perform CDA and ECDA according to the Mulliken charge population. The CDA analysis data presented in Table 4 reveal that the electron donation from TCE to β -CD or HP- β -CD (0.124 and 0.117e) is more significant than the electron back-donation from β -CD or HP- β -CD to TCE (0.010 and 0.031). ECDA analysis indicates that the net computed charges transferred from TCE to β -CD and HP- β -CD during the formation of the TCE@ β -CD and TCE@HP- β -CD complexes are 0.146 and 0.111, respectively. This suggests that charge transfer contributes to the enhancement of the stability of both complexes [61,62].

Table 4. Charge decomposition analysis (CDA) and extended charge decomposition analysis (ECDA) for TCE@ β -CD and TCE@HP- β -CD complexes.

| Complex | CDA | | | ECDA | |
|---------------------|-------|-------|-------|--------|---------------------------------|
| | d | b | d–b | r | Net Electrons Obtained by Hosts |
| TCE@ β -CD | 0.124 | 0.010 | 0.114 | –0.045 | 0.146 |
| TCE@HP- β -CD | 0.117 | 0.031 | 0.085 | –0.050 | 0.111 |

d: the number of electrons donated from TCE to β -CD or HP- β -CD. b: the number of electrons back-donated from β -CD or HP- β -CD to TCE. r: the number of electrons involved in repulsive polarization.

3.6. Monte Carlo Docking Simulations

Monte Carlo (MC) docking simulations have demonstrated their effectiveness in various molecular recognition problems [63–65]. In our study, we employed the MC method to simulate the docking of TCE within β -CD and HP- β -CD. This approach is well-suited for exploring the structural equilibrium properties of interacting complex systems. It relies on stochastically sampling a set of configurations from the Boltzmann distribution, which leads to average values of observable thermodynamic properties.

A simulation comprising approximately 500,000 structures was performed using the Amber 99 force field, which is a developed version of the Amber field (Assisted Model Building and Energy Refinement) [63,64] originally distributed by the Kollman group. Initially designed for proteins and nucleic acids, it is currently applicable to the study of macromolecules, including saccharides [65]. One of its advantages is a compromise between calculation time and result reliability, particularly for large complex systems such as the γ -cyclodextrin:C60 inclusion complex [66].

Explicit solvation was taken into consideration and periodic boundary conditions were employed to reduce edge effects. The solvation model applied is the TIP3P rigid model solvent [67] (“Transferable Intermolecular Potential 3 Points”), which involves the incorporation of pre-optimized water molecules with a force field tailored for the study of liquid water, balanced at 300 K and 1 atm [68]. The complexes were introduced into boxes of minimum dimensions with a distance between solvent–solute atoms of 2.3 Å. To save time, cut-off schemes for non-bonding interactions (electrostatic, van der Waals, etc.) were used. We chose an activated potential (switched cut-off), providing continuity for energy and forces. For the complex TCE@ β -CD, the periodic box contains 199 water molecules and its dimensions correspond to 20 Å \times 15 Å \times 20 Å. For the complex TCE@HP- β -CD, the dimensions of the box containing 219 water molecules are 21 Å \times 15 Å \times 21 Å.

Figures 5 and 6 represent the energy profiles during the simulation of TCE docking in β -CD and HP- β -CD in water, respectively, using the MC method. These profiles reveal a lowering of potential energy, due to a general tendency of the guest molecule to form the inclusion complex.

The MC process can be divided into three phases. In the initial phase (from trial 1 to 35,000), we observed a rapid decrease in energy as the guest molecule approached the CD cavity. The second phase, spanning from 35,000 to 100,000 steps, showed that the lowest average potential energy, complexation, and interaction energy were achieved for TCE@HP- β -CD. These results indicate an opening of the CD cavity, as the guest molecule attempted deeper insertion in search of a more stable conformation. Energetic values decrease weakly and slowly during this phase. From trial 100,000 to the end, the potential energy reached an equilibrium value and fluctuated around it in a stable manner. Hence, we considered these states (from 100,000) as an equilibrium status and calculated the average potential energy in this phase.

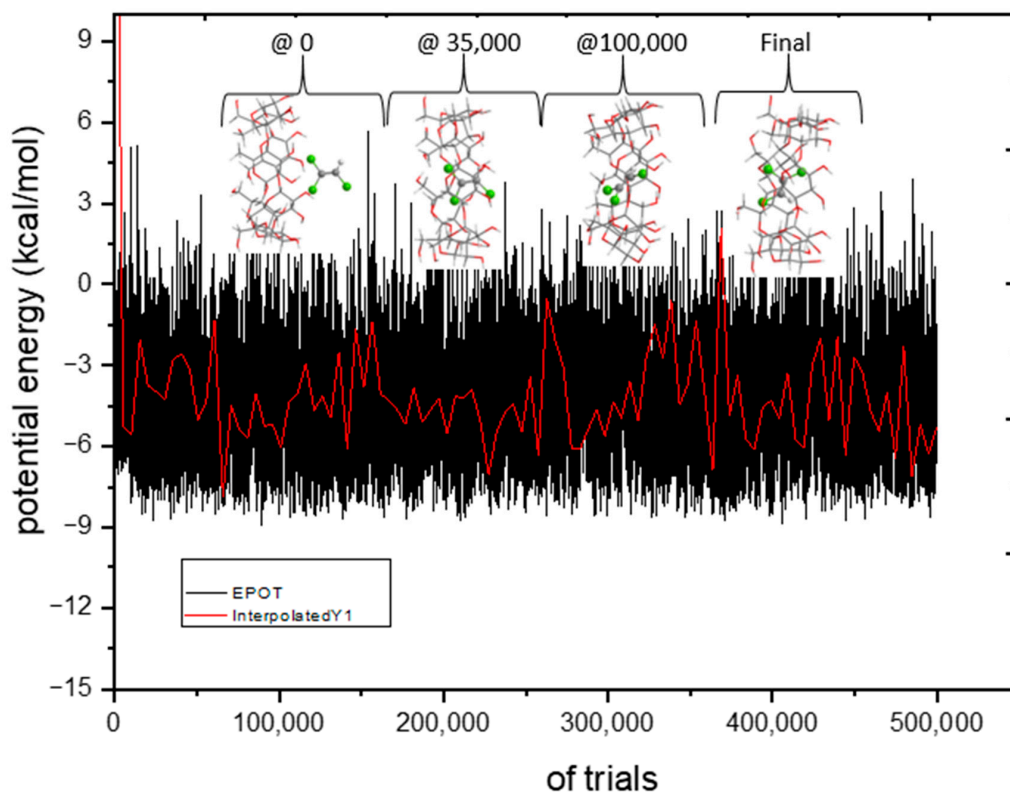


Figure 5. Calculated potential energy curves in MC simulations of TCE docking in β -CD in water. Potential energy curve (black) and interpolated values (red).

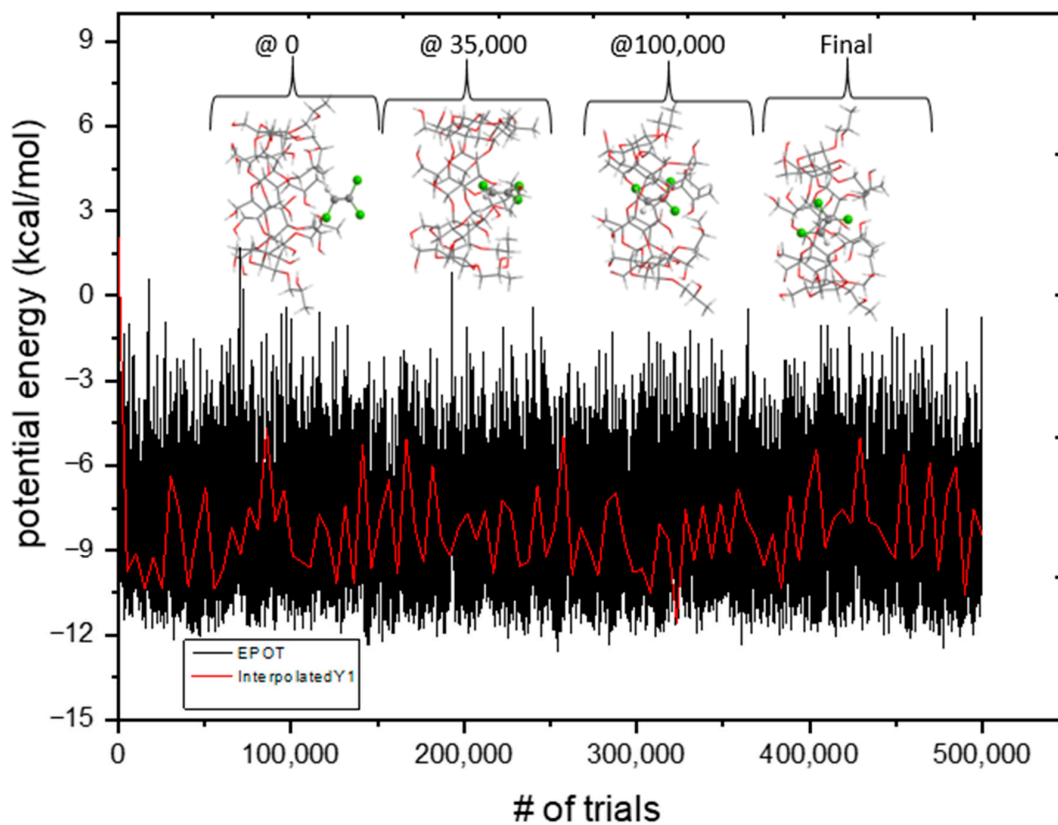


Figure 6. Calculated potential energy curves in MC simulations of TCE docking in HP- β -CD in water. Potential energy curve (black) and interpolated values (red).

The computed energy values for the inclusion complex configurations of TCE@ β -CD and TCE@HP- β -CD in the aqueous phase are summarized in Table 5. Notably, the TCE@HP- β -CD complex displayed the lowest values for its average potential energy, complexation, and interaction energies. The differences in energy between TCE@ β -CD and TCE@HP- β -CD were -3.73 kcal/mol, -2.87 kcal/mol, and -3.73 kcal/mol, respectively. Furthermore, we observed that the deformation energy of the host molecule was consistently higher than that of the guest molecule in all studied conformations. This indicates that the structure flexibility of β -CD and HP- β -CD is crucial during the formation of inclusion complexes [69].

Table 5. Energetic values computed from MC docking simulation of TCE@ β -CD and TCE@HP- β -CD complexes in water.

| | ^a $\langle E_p \rangle$ | ΔE_C | E_{int} | E_{def} (TCE) | E_{def} (β -CD) | E_{def} (HP- β -CD) |
|---------------------|------------------------------------|--------------|-----------|-----------------|--------------------------|-----------------------------|
| TCE@ β -CD | -4.79 | -26.33 | -25.20 | 0.08 | 0.49 | - |
| TCE@HP- β -CD | -8.52 | -29.20 | -28.93 | 0.13 | - | 0.89 |
| ΔE^b | -3.73 | -2.87 | -3.73 | - | - | - |

All energetic values are in kcal.mol⁻¹. ^a $\langle E_p \rangle$ is the average potential energy, with $\langle E_p \rangle = \frac{1}{2} \sum_{i=1}^n E_p$. ΔE^b is the relative energy difference of the complexes TCE@ β -CD and TCE@HP- β -CD.

4. Conclusions

The computational investigation of the host–guest inclusion process of trichloroethylene into the β -CD and HP- β -CD cavities was conducted using both the density functional theory (DFT) and Monte Carlo simulation approaches. Energetic properties analysis revealed negative complexation energies for TCE@HP- β -CD and TCE@ β -CD, reflecting the thermodynamic favorability of the process. DFT calculations using both BLYP-D4/def2-SVP-gCP and PBEh-3c showed that the complexation process is more favorable for TCE@HP- β -CD in the gas phase, whereas TCE@ β -CD exhibits more favorability for complexation in a water solvent.

Thermodynamic analysis indicated that both inclusion processes were spontaneous, exothermic, and enthalpically driven. The IGM analysis highlighted the prevalence of Van der Waals interactions as the main driving forces responsible for forming and stabilizing the TCE@HP- β -CD complex. Furthermore, Monte Carlo simulations showed an energetic preference for the TCE@HP- β -CD complex.

The electron charge density analysis revealed a charge transfer process from trichloroethylene to hydroxypropyl- β -cyclodextrin (HP- β -CD) and β -cyclodextrin (β -CD). The results of this study demonstrate the potential utility of HP- β -CD and β -CD as host systems in electronic devices, particularly in biosensors designed for the detection of TCE.

Supplementary Materials: The following supporting information can be downloaded at: <https://www.mdpi.com/article/10.3390/atoms11120153/s1>. HOMO-LUMO gaps (eV) for different considered configurations in both Modes A and B (Table S1).

Author Contributions: Conceptualization, Y.B.; methodology, S.R., Y.B. and A.B. (Abdelaziz Bouhadiba); software, Y.B. and A.B. (Abdelaziz Bouhadiba); validation, M.S., Y.B. and S.R.; formal analysis, N.S., I.B., I.O., I.M.A. and A.B. (Ahlem Benmerabet); investigation, I.O., I.B. and A.B. (Ahlem Benmerabet); resources, N.S. and S.R.; data curation, A.B. (Abdelaziz Bouhadiba) and A.B. (Ahlem Benmerabet); writing—original draft preparation, S.R., N.S., I.M.A. and Y.B.; writing—review and editing, Y.B., M.S. and A.B. (Abdelaziz Bouhadiba); visualization, A.B. (Ahlem Benmerabet) and A.B. (Abdelaziz Bouhadiba); supervision, Y.B.; project administration, S.R. and Y.B.; funding acquisition, M.S. All authors have read and agreed to the published version of the manuscript.

Funding: This research received no external funding.

Data Availability Statement: Data is contained within this article.

Conflicts of Interest: The authors declare no conflict of interest.

References

1. Antoine, R. Supramolecular Gold Chemistry: From Atomically Precise Thiolate-Protected Gold Nanoclusters to Gold-Thiolate Nanostructures. *J. Nanomater.* **2020**, *10*, 377. [CrossRef] [PubMed]
2. Fukuhara, G. Analytical supramolecular chemistry: Colorimetric and fluorimetric chemosensors. *J. Photochem. Photobiol. C Photochem. Rev.* **2020**, *42*, 100340. [CrossRef]
3. Lehn, J.-M. From supramolecular chemistry towards constitutional dynamic chemistry and adaptive chemistry. *Chem. Soc. Rev.* **2007**, *36*, 151–160. [CrossRef] [PubMed]
4. Deng, J.-H.; Luo, J.; Mao, Y.-L.; Lai, S.; Gong, Y.-N.; Zhong, D.-C.; Lu, T.-B. π - π stacking interactions: Non-negligible forces for stabilizing porous supramolecular frameworks. *Sci. Adv.* **2020**, *6*, eaax9976. [CrossRef] [PubMed]
5. Pedersen, C.J. The discovery of crown ethers. *Science* **1988**, *241*, 536–540. [CrossRef]
6. Freeman, W.A.; Mock, W.L.; Shih, N.-Y. Cucurbituril. *J. Am. Chem. Soc.* **1981**, *103*, 7367–7368. [CrossRef]
7. Del Valle, E.M. Cyclodextrins and their uses: A review. *Process Biochem.* **2004**, *39*, 1033–1046. [CrossRef]
8. Gutsche, C.D. Calixarenes. *Acc. Chem. Res.* **1983**, *16*, 161–170. [CrossRef]
9. Yadav, M.; Thakore, S.; Jadeja, R. A review on remediation technologies using functionalized Cyclodextrin. *Environ. Sci. Pollut. Res.* **2022**, *29*, 236–250. [CrossRef]
10. Gonzalez Pereira, A.; Carpena, M.; García Oliveira, P.; Mejuto, J.C.; Prieto, M.A.; Simal Gandara, J. Main applications of cyclodextrins in the food industry as the compounds of choice to form host–guest complexes. *Int. J. Mol. Sci.* **2021**, *22*, 1339. [CrossRef]
11. Aiassa, V.; Garnero, C.; Longhi, M.R.; Zoppi, A. Cyclodextrin multicomponent complexes: Pharmaceutical applications. *Pharmaceutics* **2021**, *13*, 1099. [CrossRef] [PubMed]
12. Rincón-López, J.; Almanza-Arjona, Y.C.; Riascos, A.P.; Rojas-Aguirre, Y. Technological evolution of cyclodextrins in the pharmaceutical field. *J. Drug Deliv. Sci. Technol.* **2021**, *61*, 102156. [CrossRef] [PubMed]
13. Crini, G.; Fenyvesi, É.; Sente, L. Outstanding contribution of Professor József Szejtli to cyclodextrin applications in foods, cosmetics, drugs, chromatography and biotechnology: A review. *Environ. Chem. Lett.* **2021**, *19*, 2619–2641. [CrossRef]
14. Roy, I.; Stoddart, J.F. Cyclodextrin metal–organic frameworks and their applications. *Acc. Chem. Res.* **2021**, *54*, 1440–1453. [CrossRef] [PubMed]
15. Liu, Y.; Lin, T.; Cheng, C.; Wang, Q.; Lin, S.; Liu, C.; Han, X. Research progress on synthesis and application of cyclodextrin polymers. *Molecules* **2021**, *26*, 1090. [CrossRef] [PubMed]
16. Bautista-Renedo, J.M.; Hernández-Esparza, R.; Cuevas-Yañez, E.; Reyes-Pérez, H.; Vargas, R.; Garza, J.; González-Rivas, N. Deformations of cyclodextrins and their influence to form inclusion compounds. *Int. J. Quantum Chem.* **2021**, *122*, e26859. [CrossRef]
17. Nelumdeniya, N.R.M.; Ranatunga, R.J.K.U. Complex forming behaviour of α , β and γ -cyclodextrins with varying size probe particles in silico. *Ceylon J. Sci.* **2021**, *50*, 329–339. [CrossRef]
18. Tian, B.; Hua, S.; Tian, Y.; Liu, J. Cyclodextrin-based adsorbents for the removal of pollutants from wastewater: A review. *Environ. Sci. Pollut. Res.* **2021**, *28*, 1317–1340. [CrossRef]
19. Majd, M.; Yazdanpanah, M.; Bayatloo, M.R.; Nojavan, S. Recent advances and applications of cyclodextrins in magnetic solid phase extraction. *Talanta* **2021**, *229*, 122296. [CrossRef]
20. Kim, J.S.; Choi, Y.J.; Woo, M.R.; Cheon, S.; Ji, S.H.; Im, D.; Ud Din, F.; Kim, J.O.; Youn, Y.S.; Oh, K.T.; et al. New potential application of hydroxypropyl- β -cyclodextrin in solid self-nanoemulsifying drug delivery system and solid dispersion. *Carbohydr. Polym.* **2021**, *271*, 118433. [CrossRef]
21. Oba, B.T.; Zheng, X.; Aborisade, M.A.; Liu, J.; Yohannes, A.; Kavwenje, S.; Sun, P.; Yang, Y.; Zhao, L. Remediation of trichloroethylene contaminated soil by unactivated peroxymonosulfate: Implication on selected soil characteristics. *J. Environ. Manag.* **2021**, *285*, 112063. [CrossRef] [PubMed]
22. Liu, Y.; Chen, H.; Zhao, L.; Li, Z.; Yi, X.; Guo, T.; Cao, X. Enhanced trichloroethylene biodegradation: Roles of biochar-microbial collaboration beyond adsorption. *Sci. Total Environ.* **2021**, *792*, 148451. [CrossRef] [PubMed]
23. Huang, Y.; Xia, Y.; Tao, Y.; Jin, H.; Ji, C.; Aniagu, S.; Chen, T.; Jiang, Y. Protective effects of resveratrol against the cardiac developmental toxicity of trichloroethylene in zebrafish embryos. *Toxicology* **2021**, *452*, 152697. [CrossRef] [PubMed]
24. Agency for Toxic Substances and Disease Registry (ATSDR). ATSDR's Substance Priority List. 2017. Available online: https://www.atsdr.cdc.gov/spl/resources/2017_atsdr_substance_priority_list.html (accessed on 19 July 2022).
25. Love, O.T., Jr.; Eilers, R.G. Treatment of drinking water containing trichloroethylene and related industrial solvents. *J.-Am. Water Works Assoc.* **1982**, *74*, 413–425. [CrossRef]
26. Hennebel, T.; Simoen, H.; De Windt, W.; Verloo, M.; Boon, N.; Verstraete, W. Biocatalytic dechlorination of trichloroethylene with bio-palladium in a pilot-scale membrane reactor. *Biotechnol. Bioeng.* **2009**, *102*, 995–1002. [CrossRef] [PubMed]
27. Sun, L.; Xu, G.; Tu, Y.; Zhang, W.; Hu, X.; Yang, P.; Xie, X. Multifunctional porous β -cyclodextrin polymer for water purification. *Water Res.* **2022**, *222*, 118917. [CrossRef] [PubMed]
28. Wang, Z.; Li, T.T.; Peng, H.K.; Ren, H.T.; Lou, C.W.; Lin, J.H. Low-cost hydrogel adsorbent enhanced by trihydroxy melamine and β -cyclodextrin for the removal of Pb (II) and Ni (II) in water. *J. Hazard. Mater.* **2021**, *411*, 125029. [CrossRef] [PubMed]
29. Sun, Z.; Wang, M.; Mu, X.; Zhou, J.; Ke, X.; Wu, Q.; Miao, L. Sustainable β -cyclodextrin modified polyacrylamide hydrogel for highly efficient solar-driven water purification. *Mater. Today Energy* **2023**, *35*, 101330. [CrossRef]

30. Morin-Crini, N.; Crini, G. Environmental applications of water-insoluble β -cyclodextrin-epichlorohydrin polymers. *Prog. Polym. Sci.* **2013**, *38*, 344–368. [CrossRef]
31. Mahmood, A.; Khan, S.U.-D.; Ur Rehman, F. Assessing the quantum mechanical level of theory for prediction of UV/Visible absorption spectra of some aminoazobenzene dyes. *J. Saudi Chem. Soc.* **2015**, *19*, 436–441. [CrossRef]
32. Chermette, H.J. Chemical reactivity indexes in density functional theory. *Comput. Chem.* **1999**, *20*, 129–154. [CrossRef]
33. Belhocine, Y.; Bouhadiba, A.; Rahim, M.; Nouar, L.; Djilani, I.; Khatmi, D.I. Inclusion Complex Formation of β -Cyclodextrin with the Nonsteroidal Anti-inflammatory Drug Flufenamic Acid: Computational Study. *Macroheterocycles* **2018**, *11*, 203–209. [CrossRef]
34. Belhocine, Y.; Rahali, S.; Allal, H.; Assaba, I.M.; Ghoniem, M.G.; Ali, F.A.M. A dispersion corrected DFT investigation of the inclusion complexation of dexamethasone with β -cyclodextrin and molecular docking study of its potential activity against COVID-19. *Molecules* **2021**, *26*, 7622. [CrossRef] [PubMed]
35. Shirin, S.; Buncel, E.; vanLoon, G.W. The use of beta-cyclodextrins to enhance the aqueous solubility of trichloroethylene and perchloroethylene and their removal from soil organic matter: Effect of substituents. *Can. J. Chem.* **2003**, *81*, 45–52. [CrossRef]
36. Kashiyama, N.; Boving, T.B. Hindered gas-phase partitioning of trichloroethylene from aqueous cyclodextrin systems: Implications for treatment and analysis. *Environ. Sci. Technol.* **2004**, *38*, 4439–4444. [CrossRef]
37. Liang, C.; Huang, C.; Mohanty, N.; Lu, C.J.; Kurakalva, R.M. Hydroxypropyl-beta-cyclodextrin-mediated iron-activated persulfate oxidation of trichloroethylene and tetrachloroethylene. *Ind. Eng. Chem. Res.* **2007**, *46*, 6466–6479. [CrossRef]
38. Khan, N.A.; Johnson, M.D.; Carroll, K.C. Spectroscopic Methods for Aqueous Cyclodextrin Inclusion Complex Binding Measurement for 1,4-Dioxane, Chlorinated Co-Contaminants, and Ozone. *J. Contam. Hydrol.* **2018**, *210*, 31–41. [CrossRef]
39. Neese, F. The ORCA program system. *Wiley Interdiscip. Rev. Comput. Mol. Sci.* **2012**, *2*, 73–78. [CrossRef]
40. Neese, F.; Wennmohs, F.; Becker, U.; Riplinger, C. The ORCA quantum chemistry program package. *J. Chem. Phys.* **2020**, *152*, 224108. [CrossRef]
41. Aree, T.; Chaichit, N. Crystal structure of β -cyclodextrin-benzoic acid inclusion complex. *Carbohydr. Res.* **2003**, *338*, 439–446. [CrossRef]
42. Becke, A.D. Density-functional exchange-energy approximation with correct asymptotic behavior. *Phys. Rev. A* **1988**, *38*, 3098–3100. [CrossRef] [PubMed]
43. Lee, C.; Yang, W.; Parr, R.G. Development of the Colle-Salvetti correlation-energy formula into a functional of the electron density. *Phys. Rev. B* **1988**, *37*, 785–789. [CrossRef] [PubMed]
44. Caldeweyher, E.; Ehlert, S.; Hansen, A.; Neugebauer, H.; Spicher, S.; Bannwarth, C.; Grimme, S. A generally applicable atomic-charge dependent London dispersion correction. *J. Chem. Phys.* **2019**, *150*, 154122. [CrossRef] [PubMed]
45. Kruse, H.; Grimme, S.A. geometrical correction for the inter-and intra-molecular basis set superposition error in Hartree-Fock and density functional theory calculations for large systems. *J. Chem. Phys.* **2012**, *136*, 154101. [CrossRef] [PubMed]
46. Liu, L.; Guo, Q.X. Use of quantum chemical methods to study cyclodextrin chemistry. *J. Incl. Phenom. Macrocycl. Chem.* **2004**, *50*, 95–103. [CrossRef]
47. Jmol: An Open-Source Java Viewer for Chemical Structures in 3D. Available online: <http://www.jmol.org> (accessed on 3 August 2022).
48. Dapprich, S.; Frenking, G. Investigation of donor-acceptor interactions: A charge decomposition analysis using fragment molecular orbitals. *J. Phys. Chem.* **1995**, *99*, 9352–9362. [CrossRef]
49. Xiao, M.; Lu, T. Generalized Charge Decomposition Analysis (GCDA) Method. *J. Adv. Phys. Chem.* **2015**, *4*, 111–124. [CrossRef]
50. Gorelsky, S.I.; Ghosh, S.; Solomon, E.I. Mechanism of N₂O reduction by the μ -S tetranuclear CuZ cluster of nitrous oxide reductase. *J. Am. Chem. Soc.* **2006**, *128*, 278–290. [CrossRef]
51. Lefebvre, C.; Rubez, G.; Khartabil, H.; Boisson, J.C.; Contreras-García, J.; Hénon, E. Accurately extracting the signature of intermolecular interactions present in the NCI plot of the reduced density gradient versus electron density. *Phys. Chem. Chem. Phys.* **2017**, *19*, 17928–17936. [CrossRef]
52. Lu, T.; Chen, F. Multiwfn: A multifunctional wavefunction analyzer. *J. Comput. Chem.* **2012**, *33*, 580–592. [CrossRef]
53. Humphrey, W.; Dalke, A.; Schulten, K. VMD: Visual molecular dynamics. *J. Mol. Graph.* **1996**, *14*, 33–38. [CrossRef] [PubMed]
54. Grimme, S.; Brandenburg, J.G.; Bannwarth, C.; Hansen, A. Consistent structures and interactions by density functional theory with small atomic orbital basis sets. *J. Chem. Phys.* **2015**, *143*, 054107. [CrossRef] [PubMed]
55. Marenich, A.V.; Cramer, C.J.; Truhlar, D.G. Universal solvation model based on solute electron density and on a continuum model of the solvent defined by the bulk dielectric constant and atomic surface tensions. *J. Phys. Chem. B* **2009**, *113*, 6378–6396. [CrossRef] [PubMed]
56. Hanwell, M.D.; Curtis, D.E.; Lonie, D.C.; Vandermeersch, T.; Zurek, E.; Hutchison, R.G. Avogadro: An advanced semantic chemical editor, visualization, and analysis platform. *J. Cheminform.* **2012**, *4*, 17. [CrossRef] [PubMed]
57. Lu, T.; Chen, Q. Independent Gradient Model Based on Hirshfeld Partition: A New Method for Visual Study of Interactions in Chemical Systems. *J. Comput. Chem.* **2022**, *43*, 539–555. [CrossRef]
58. Mesri, N.; Belhocine, Y.; Messikh, N.; Sayede, A.; Mouffok, B. Molecular DFT Investigation on the Inclusion Complexation of Benzo [a] pyrene with γ -Cyclodextrin. *Macroheterocycles* **2021**, *14*, 164–170. [CrossRef]
59. Messiad, F.A.; Ammouchi, N.; Belhocine, Y.; Alhussain, H.; Ghoniem, M.G.; Said, R.B.; Ali, F.A.M.; Rahali, S. In Search of Preferential Macrocyclic Hosts for Sulfur Mustard Sensing and Recognition: A Computational Investigation through the New Composite Method r2SCAN-3c of the Key Factors Influencing the Host-Guest Interactions. *Nanomaterials* **2022**, *12*, 2517. [CrossRef]

60. Kabouche, Z.; Belhocine, Y.; Benlecheb, T.; Assaba, I.M.; Litim, A.; Lalalou, R.; Mechhoud, A. A DFT-D4 investigation of the complexation phenomenon between pentachlorophenol and β -cyclodextrin. *Chim. Techno Acta* **2023**, *10*, 202310209. [[CrossRef](#)]
61. Litim, A.; Belhocine, Y.; Benlecheb, T.; Ghoniem, M.G.; Kabouche, Z.; Ali, F.A.M.; Abdulkhair, B.Y.; Seydou, M.; Rahali, S. DFT-D4 Insight into the Inclusion of Amphetamine and Methamphetamine in Cucurbituril: Energetic, Structural and Biosensing Properties. *Molecules* **2021**, *26*, 7479. [[CrossRef](#)]
62. Assaba, I.M.; Rahali, S.; Belhocine, Y.; Allal, H. Inclusion complexation of chloroquine with α and β -cyclodextrin: Theoretical insights from the new B97-3c composite method. *J. Mol. Struct.* **2021**, *1227*, 129696. [[CrossRef](#)]
63. Weiner, S.J.; Kollman, P.A.; Singh, U.C.; Case, D.A.; Ghio, C.; Alagona, G.; Profeta, S.; Weiner, P. A New Force Field for Molecular Mechanical Simulation of Nucleic Acids and Proteins. *J. Am. Chem. Soc.* **1984**, *106*, 765–784. [[CrossRef](#)]
64. Weiner, S.J.; Kollman, P.A.; Nguyen, D.T.; Case, D.A. An all atom force field for simulations of proteins and nucleic acids. *J. Comput. Chem.* **1986**, *7*, 230–252. [[CrossRef](#)] [[PubMed](#)]
65. Pearlman, D.A.; Case, D.A.; Caldwell, J.W.; Ross, W.S.; Cheatham, T.E., III; DeBolt, S.; Ferguson, D.; Seibel, G.; Kollman, P. AMBER, a package of computer programs for applying molecular mechanics, normal mode analysis, molecular dynamics and free energy calculations to simulate the structural and energetic properties of molecules. *Comput. Phys. Commun.* **1995**, *91*, 1–41. [[CrossRef](#)]
66. Bonnet, P.; Beà, I.; Jaime, C.; Morin-Allory, L. Molecular Modelling Study of the 2:1 γ -Cyclodextrin:C60 Complex. Dummy Atoms Simulating Bond Electron Distribution. *Supramol. Chem.* **2003**, *15*, 251–260. [[CrossRef](#)]
67. Jorgensen, W.L.; Chandrasekhar, J.; Madura, J.D.; Impey, R.W.; Klein, M.L. Comparison of Simple Potential Functions for Simulating Liquid Water. *J. Chem. Phys.* **1983**, *79*, 926–935. [[CrossRef](#)]
68. *Hyperchem, Release. 7.51 for Windows MM System*; Hypercube, Inc.: Gainesville, FL, USA, 2002.
69. Murthy, C.N.; Geckeler, K.E. Stability studies on the water-soluble β -cyclodextrin–Fullerene inclusion complex. *Fuller. Nanotub. Carbon Nanostruct.* **2002**, *10*, 91–98. [[CrossRef](#)]

Disclaimer/Publisher’s Note: The statements, opinions and data contained in all publications are solely those of the individual author(s) and contributor(s) and not of MDPI and/or the editor(s). MDPI and/or the editor(s) disclaim responsibility for any injury to people or property resulting from any ideas, methods, instructions or products referred to in the content.